frontiers | Frontiers in Food Science and Technology

ORIGINAL RESEARCH
published: 14 June 2022
doi: 10.3389/frfst.2022.889360

Probing Prolamin-Anthocyanin Interactions for the Rational Design of Plant-Based Encapsulation Systems

Joshua W. Salamun[1], *Aicheng Chen*[2], *Maria G. Corradini*[1,3]* *and Iris J. Joye*[1]*

[1]Department of Food Science, University of Guelph, Guelph, ON, Canada, [2]Department of Chemistry, University of Guelph, Guelph, ON, Canada, [3]Arrell Food Institute, University of Guelph, Guelph, ON, Canada

OPEN ACCESS

Edited by:
Viridiana Tejada-Ortigoza, Monterrey Institute of Technology and Higher Education (ITESM), Mexico

Reviewed by:
Ninganagouda R. Patil, B V B College of Engineering and Technology, India
Néstor Gutiérrez-Méndez, Autonomous University of Chihuahua, Mexico

***Correspondence:**
Maria G. Corradini
mcorradi@uoguelph.ca
Iris J. Joye
ijoye@uoguelph.ca

Specialty section:
This article was submitted to Food Biotechnology, a section of the journal Frontiers in Food Science and Technology

Received: *04 March 2022*
Accepted: *05 May 2022*
Published: *14 June 2022*

Citation:
Salamun JW, Chen A, Corradini MG and Joye IJ (2022) Probing Prolamin-Anthocyanin Interactions for the Rational Design of Plant-Based Encapsulation Systems. Front. Food. Sci. Technol. 2:889360. doi: 10.3389/frfst.2022.889360

Plant proteins are increasingly focused upon as alternatives to animal-derived macromolecules for the encapsulation of bioactives. The rational design of encapsulation carriers should be based on a solid understanding of the interactions between the proteins and bioactives. Encapsulation technology for food applications has focused predominantly on the protection and controlled release of hydrophobic bioactives. For hydrophilic molecules, although not less important from a nutritional and health perspective, significantly fewer encapsulation systems have been explored, designed and described. As hydrophilic molecules tend to partition into the aqueous food matrix, it is even more crucial to understand and to be able to modulate the interactions between the hydrophilic bioactive and the encapsulating matrix material in food relevant conditions. Therefore, examining the nature of the interactions between anthocyanins (ACNs), a hydrophilic bioactive, and prolamin plant proteins (gliadin, hordein, secalin, and avenin) is timely. These interactions were examined using steady-state and time-resolved luminescence spectroscopy techniques. The ACN-induced quenching of the prolamins intrinsic fluorescence emission did not follow a linear Stern-Volmer relationship, but rather displayed an upward curvature for all the prolamins tested. Hence, both static and dynamic quenching likely occurred in the prolamin-ACN systems. The quenching mechanism was further explored based on the changes in fluorescence lifetime as ACN concentration increased. As the independent lifetimes of the prolamin-ACN combinations did not decrease discernibly as a function of ACN concentration, static quenching is presumably the predominant quenching mechanism. The thermodynamic parameters revealed that the interactions between secalin- and avenin-ACN are mainly driven by the hydrophobic effect, while those between gliadin- and hordein-ACN are dominated by ionic interactions. Zeta-potential measurements support the dominant ionic interactions found for gliadin and hordein. The insights gained in this research will serve as a sound basis for further studies focusing on matrix selection with regard to creating performant encapsulation systems for ACNs.

Keywords: protein, encapsulation, anthocyanin, fluorescence, food, prolamin

INTRODUCTION

Anthocyanins (ACNs) are natural water-soluble plant pigments, which give red, blue, or purple colors to many fruits and flowers (Prior and Wu, 2006; Chung et al., 2015; Burton-Freeman et al., 2016). Besides their potential use as natural colorants in food, ACNs are also potent antioxidants (Viljanen et al., 2005; Burton-Freeman et al., 2016). The ACN structure includes a central flavylium cation (anthocyanidin core) that is glycosylated and acylated (Prior and Wu, 2006; Chung et al., 2015). While ACNs are associated with desirable functional properties and a variety of health benefits (Zhao et al., 2004; Forester and Waterhouse, 2008; Tressera-Rimbau et al., 2014; Cassidy et al., 2016; Kimble et al., 2018), they are highly susceptible to chemical degradation, leading to discoloration and loss of their bioactive properties (Chung et al., 2015; Cassidy et al., 2016; Kimble et al., 2018). Chemical degradation is hastened by exposure to high temperatures, elevated pH conditions, and the presence of certain components, such as ascorbic acid, enclosed in the food matrix (Hubbermann et al., 2006; Sui et al., 2014; Chung et al., 2015). Encapsulation is one of several strategies routinely explored to enhance the stability of labile bioactive compounds and to increase ACNs performance when used as natural food colorants (Arangoa et al., 2001; Wong et al., 2012; He et al., 2016).

Prolamin particles have shown to be promising plant-based encapsulation systems for bioactive molecules (Patel et al., 2012; Joye et al., 2015; Xiao et al., 2015). In addition, particles made up of gliadin, *i.e.*, wheat prolamin, display bioadhesive properties, which are believed to prolong their residence time in the gastrointestinal tract (Arangoa et al., 2001). Extended residence time usually increases the efficiency of a carrier for controlled release and target delivery of bioactives in the gastrointestinal tract (Arangoa et al., 2001). Gaining insights into the nature of the interactions between ACNs and prolamins is crucial for assessing ACN encapsulation, controlled release and retention efficiency of prolamin-based colloidal systems. Due to the hydrophilic nature of ACNs, the encapsulation and retention of these bioactives in the encapsulation matrix could exhibit additional challenges relative to what is experienced with hydrophobic bioactives.

Fluorescence quenching studies are often used to assess the nature and extent of the interactions between proteins and bioactive compounds, including polyphenols (Lakowicz, 2006; Skrt et al., 2012; Keppler et al., 2014; Joye et al., 2015). Fluorescence quenching, i.e., decrease of fluorescence intensity, in these studies is driven by a variety of processes such as energy transfer due to molecular interactions among protein segments or between the protein and the quencher or formation of ground-state complexes between the fluorophore and quencher molecules, or collisional quenching (Lakowicz, 2006). Static quenching often involves the formation of non-fluorescent complexes between the quencher and fluorophore, while dynamic quenching refers to non-radiative decay triggered by the collision between the two molecules (Lakowicz, 2006; Joye et al., 2015). Fluorescence quenching studies on interactions between prolamin proteins and polyphenols generally focus on the Trp fluorescence of prolamin proteins. Skrt et al. (2012) explored the interactions between various catechins, flavones and hydroxycinnamic acids, and bovine serum albumin through fluorescence quenching. They found that the binding affinity between esterified catechins and the protein is higher, while it is the lowest for epigallocatechin, compared with the other polyphenols included in their study. Similarly, Joye et al. (2015) investigated the complexation of resveratrol to zein and gliadin through fluorescence quenching. Based on the thermodynamic data, these researchers concluded that while the interaction between (the more hydrophobic) zein and resveratrol is dominated by the hydrophobic effect, the interactions between gliadin and resveratrol are mainly stabilized by hydrogen bonds. However, no in-depth study of the interaction between ACN and different prolamins has been published. The focus on ACN and prolamins is justifiable due to their economic potential and scientific value as natural (but unstable) colorants (ACN) and as protective encapsulation vehicles for bioactives (prolamins) for food applications. Therefore, the purpose of this study was to explore the nature of the interaction between ACNs from bilberry extract (BE) (mainly delphinidin-derivatives) and several prolamin proteins (i.e., gliadin, hordein, secalin and avenin) using steady-state and time-resolved fluorescence spectroscopic techniques. The gained insights should build a sound basis for further studies focusing on prolamin matrix selection with regard to creating highly performant and tunable encapsulation systems for ACNs.

MATERIALS AND METHODS

Materials

Commercial wheat gluten was purchased from Bulk Barn (Bulk Barn Foods, Aurora, ON, Canada). Barley and oats were from Wintermar Farms (West Montrose, ON, Canada), while rye was donated by the Department of Plant Sciences of the University of Guelph (Guelph, ON, Canada). Barley, rye, and oats wholemeal samples were prepared by grinding barley, rye, and oats using a UDY mill (UDY Corporations, Fort Collins, CO, United States) with a 0.50 mm screen. BE was purchased from Evergreen Biotech Inc. (Xian, China). All chemicals, reagents, and solvents were of analytical grade and purchased from Fisher Scientific (Mississauga, ON, Canada).

Extraction of Prolamins

Prolamin proteins were extracted from commercial wheat gluten, barley, rye, and oats wholemeal by suspending 100 g of these powders in 400 ml 70% (v/v) aqueous ethanol. The suspensions were stirred for 2 h at room temperature prior to being centrifuged for 10 min at 10,000 *g* using an Allegra X-15R centrifuge (Beckman Coulter Inc., Indianapolis, IN, United States). The supernatants were vacuum filtered using Q5 Fisherbrand filter paper (ThermoFisher Scientific, Mississauga, ON, Canada) and then left overnight at 4°C to allow insoluble material to sediment, prior to being centrifuged (10,000 *g* for 10 min) and vacuum filtered (using Q5 Fisherbrand filter paper) for a second time. The final gliadin, hordein, secalin, and avenin extracts contained about 9.3, 1.0, 0.9, and 0.6% (w/v) protein as determined by DUMAS analysis (Leco FP-528, Leco Inc., St. Joseph, MI, United States).

Steady-State Fluorescence Spectroscopy

Ethanol/acetate buffer mixtures were prepared by combining ethanol with sodium acetate buffer (pH 4.5, 0.100 M) at a 7:3 volume ratio. A protein concentration study was conducted for each prolamin prior to the quenching experiments. The protein concentration was optimized to ensure enough fluorescence emission while preventing the inner filter effect, i.e., re-absorbance of the emission due to excessive concentration of the fluorophore. Based on the results of the protein concentration study, for subsequent measurements, the prolamin extracts were diluted with the ethanol/acetate buffer mixture to reach the optimized protein concentration of 0.017, 0.018, 0.010, and 0.005 (w/v) for gliadin, hordein, secalin, and avenin, respectively. A 0.030% (w/v) BE solution was prepared by dissolving the BE powder in the ethanol/acetate buffer mixture. The BE solutions were then filtered using a 0.45 um syringe filter (Thermo Fisher Scientific, Mississauga, ON, Canada). Solutions with different BE concentrations (i.e., quencher) were mixed with the protein solutions, while keeping the protein concentration constant (i.e., optimized protein concentration). The BE concentration in the quenching experiments varied between 0 and 4.86×10^{-2} mM.

Steady-state fluorescence measurements were performed using a Shimadzu RF-5301PC spectrofluorimeter (Shimadzu Scientific Instruments Inc., Kyoto, Japan). Measurements were performed at five different temperatures (15, 20, 25, 30 and 35°C). In all experiments, the slit width (excitation and emission) was set at 3 nm. The excitation wavelength was set at 280 nm, and the prolamins emission signal was collected from 290 to 450 nm.

Time-Resolved Fluorescence Spectroscopy

Fluorescence lifetimes measurements were carried out using a Time-Correlated Single-Photon Counting (TCSPC) accessory on a Fluoromax Plus C spectrophotometer (Horiba Jobin Yvon, Kyoto, Japan) using a 283 nm nanoLED as the light source. The sample preparation was the same as described previously for the steady-state fluorescence measurements. 0.04% (w/v) LUDOX was used as a scatterer to measure the instrument response function (IRF). The decays were analyzed using DAS-6 decay analysis software. The lifetimes were calculated using a multi exponential approach and the non-extensive distribution (NED) method as programmed within the DAS software (Horiba Scientific, Edison, NJ, United States). The goodness of fit of the decay data was assessed using the χ^2 criteria (i.e., fits with $\chi^2 \sim 1.00$ were considered good and >1.20 were discarded) and visual inspection of the residuals (i.e., residuals should be randomly distributed around zero and within the range of few standard deviations).

Zeta-Potential Analysis

Zeta-potential values were measured using laser Doppler electrophoresis (Zetasizer Nano ZS, Malvern Instruments Ltd., Worcestershire, United Kingdom). Samples were transferred to a disposable capillary-cell (Malvern Instruments Ltd., Worcestershire, United Kingdom) prior to the measurement. All proteins were solubilized in 70% aqueous ethanol. Gliadin and hordein were analyzed at a concentration of 1.0% (w/v), while secalin and avenin were analyzed at 0.9 and 0.6% (w/v), respectively. All measurements were conducted at 25°C.

Reverse-Phase High Performance Liquid Chromatography

Gliadin extract was diluted to 1.0% (w/v) using 70% (v/v) aqueous ethanol, while the other prolamin extracts were kept at their final extracted concentrations [i.e., 1.0, 0.9, and 0.6% (w/v) for hordein, secalin and avenin, respectively]. The separation of the proteins in the prolamin extracts was performed using a Gemini-NX-C18 column (Gemini 5 um C18 110 A, 250 × 4.6 mm) on a modular LC-10 HPLC system (Shimadzu, Kyoto, Japan). The detector wavelength was set at 214 nm and the injection volume for the extracts was 20 uL. A binary gradient profile was used for sample elution. Eluent A was MilliQ-water, to which trifluoroacetic acid (TFA) [0.1% (v/v)] was added. Eluent B was acetonitrile (ACN), to which also TFA [0.1% (v/v)] was added. A linear gradient from 20 to 56% (v/v) eluent B over 60 min was used to separate the proteins based on their polarity. The gradient elution program was run at a constant flow rate of 0.8 mL/min, and the column oven was set at 50°C.

Statistical Analysis

All samples were prepared in triplicate unless stated otherwise. The results are reported as mean values with accompanying standard deviations represented by error bars in all figures. To assess the significance of results obtained, one-way analysis of variance (ANOVA) was performed on the data sets, followed by Tukeys post-hoc test, both at a significance level of $p < 0.05$. The fluorescence spectra collected for the fluorescence quenching study were normalized based on each prolamin's maximum Trp fluorescence intensity in the absence of ACNs.

RESULTS

Prolamin Fluorescence Energy and Intensity

The fluorescence spectra of gliadin and secalin displayed two peaks (λ_{em}^{max} 305 and 340 nm), corresponding to Tyr and Trp fluorescence (**Supplementary Figure S1**). In contrast, the intrinsic fluorescence spectra of avenin and hordein only showed a Trp fluorescence signal at λ_{em}^{max} 340 and 330 nm, respectively (**Supplementary Figure S1**). Although the Tyr concentration in prolamins is higher than their respective Trp concentration (Belitz et al., 2004), the intensity of the Tyr emission peak (~305 nm) was consistently lower than that of Trp (~340 nm). The lower emission intensity of Tyr recorded from the prolamin solutions can be attributed to the fluorescence resonance energy transfer (FRET) from Tyr to Trp, since Tyr-Trp are a well-known and efficient FRET donor/acceptor pair (Lakowicz, 1999; Paul et al., 2013; Ghisaidoobe and Chung, 2014). Due to FRET, the intensity of the Trp fluorescence emission was the highest recorded; its corresponding peak was thus evaluated during the quenching experiments. In each of

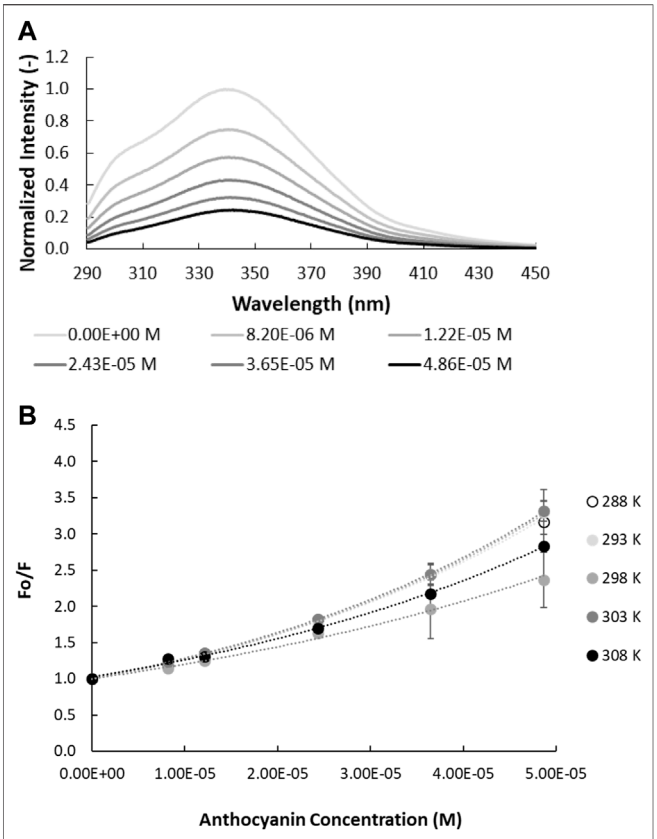

FIGURE 1 | Quenching of intrinsic gliadin fluorescence by anthocyanins. **(A)** Fluorescence spectra of gliadin (0.017% w/v; λex = 280 nm; pH = 4.50 in ethanol/acetate buffer, 298 K as function of anthocyanin concentration. **(B)** Relative intrinsic fluorescence of gliadin fluorescence as a function of anthocyanin concentration. The temperature at which the experiment is carried out is specified in the legend.

these prolamin samples, however, different populations of Trp are present. These Trp populations differ in their location along the amino acid sequence and the local environment in the folded protein structure. The spectra recorded for each of the prolamin samples are, hence, a cumulative signal of different Trp populations. These different Trp populations differ in their fluorescence intensity and maximum emission wavelength depending on the rigidity and solvation around the amino acid within the protein. The concentration of gliadin, hordein, secalin, and avenin extracts was optimized for the Trp fluorescence quenching experiments at 0.017, 0.018 0.010, and 0.005 (w/v), respectively.

Quenching of Protein Fluorescence Intensity by ACN: Steady State Measurements

Fluorescence emission spectra, measured at an excitation wavelength of 280 nm, were recorded for all prolamins (i.e., gliadin, hordein, secalin, and avenin) as a function of increasing BE concentration (**Figure 1A**, **Supplementary Figure S2**). Trp fluorescence quenching increased with increasing concentration of ACNs. As outlined above, fluorescence quenching can either be dynamic, resulting from the collision between fluorophore and quencher, or static, originating from the formation of ground state complexes between the fluorophore and quencher (Lakowicz, 2006; Joye et al., 2015).

Fluorescence quenching can be described by the Stern-Volmer equation:

$$\frac{F_0}{F} = 1 + K_q \tau_0 [Q] = 1 + K_{sv}[Q] \quad (1)$$

where F_0 and F are the fluorescence emission intensity of the prolamin in the absence and presence of quencher, respectively, K_q is the bimolecular quenching constant, τ_0 is the lifetime of fluorescence in the absence of quencher, [Q] is the concentration of quencher, and K_{sv} is the Stern-Volmer quenching constant. The mechanisms of ACN-induced quenching of the intrinsic fluorescence emission of the prolamins can be deduced from the Stern-Volmer plots (**Figure 1B**, **Supplementary Figure S3**). Linearity of the Stern-Volmer plots is indicative of either pure static or dynamic quenching, which can be differentiated based on the changes in the slope triggered by an increase of temperature. The Stern-Volmer plots for gliadin, avenin, hordein, and secalin, however, deviated from linearity, showing an upward concavity. This is a characteristic feature of simultaneous static and dynamic quenching (Lakowicz, 1999; Paul et al., 2013) and has been previously observed in anthocyanin-protein quenching experiments (Wang and Xie, 2019; Ren and Giusti, 2021). Ren and Giusti (2021) ascribed the non-linearity to the use of an ACN mixture, rather than focusing on a pure anthocyanin sample. As the BE extract is essentially also a mixture of ACNs, this might have caused the non-linearity in the here presented data too. Guo et al. (2022), however, studied the interactions between gliadin and grape skin ACN extract, essentially a mixture of ACNs, and did obtain linear Stern-Volmer plots. Time-resolved fluorescence spectroscopic measurements were, hence, needed to effectively explore the nature of the quenching mechanism observed between gliadin, hordein, secalin and avenin, on the one hand, and ACNs, on the other hand.

Time-Resolved Fluorescence Measurements

Nanosecond resolved fluorescence decay profiles of all prolamins $\lambda_{ex} = 283nm, \lambda_{em} = \lambda_{em}^{\max}$ (**Supplementary Figure S4**) at varying concentrations of ACNs (0 - 4.86×10^{-2} mM) were recorded and characterized using a multi-exponential model:

$$I(t) = I(0) * \sum_{i=1}^{n} \alpha_i \exp\left(-\frac{t}{\tau_i}\right) \quad (2)$$

where α_i is the pre-exponential decay factor or relative amplitude corresponding to the i^{th} decay time constant, τ_i (Lakowicz, 1999;

TABLE 1 | Time-resolved fluorescence decay parameters of gliadin in the presence of increasing anthocyanin concentration (λ_{ex} = 280 *nm*, λ_{em} = 340 *nm*).

Samples	τ_1 (ns)	τ_2 (ns)	τ_3 (ns)	χ^2	τ_{a0} [a]
Gliadin	1.34 ± 0.03a	4.15 ± 0.05a	10.11 ± 0.16a	1.17 ± 0.02	3.54 ± 0.04 a
Gliadin +8.20E-06 M anthocyanins	1.13 ± 0.09b	3.95 ± 0.17ab	21.71 ± 8.18b	1.11 ± 0.02	3.53 ± 0.10 ab
Gliadin +1.22E-05 M anthocyanins	1.18 ± 0.10ab	4.13 ± 0.09a	13.50 ± 3.05ab	1.13 ± 0.03	3.59 ± 0.11 a
Gliadin +2.43E-05 M anthocyanins	1.02 ± 0.08bc	4.01 ± 0.20ab	15.32 ± 0.29ab	1.16 ± 0.04	3.46 ± 0.03 abc
Gliadin +3.65E-05 M anthocyanins	0.92 ± 0.07c	3.89 ± 0.07ab	16.77 ± 4.31ab	1.13 ± 0.02	3.37 ± 0.09 bc
Gliadin +4.86E-05 M anthocyanins	0.83 ± 0.01c	3.69 ± 0.05b	18.94 ± 2.48ab	1.16 ± 0.01	3.25 ± 0.02 c

τ_i are the lifetimes components estimated when fitting the decays with ***Eq. 2****, τ_{a0} is the amplitude-weighted average lifetime.*
[a]*Samples with different letters are significantly different at* $\alpha = 0.05$.

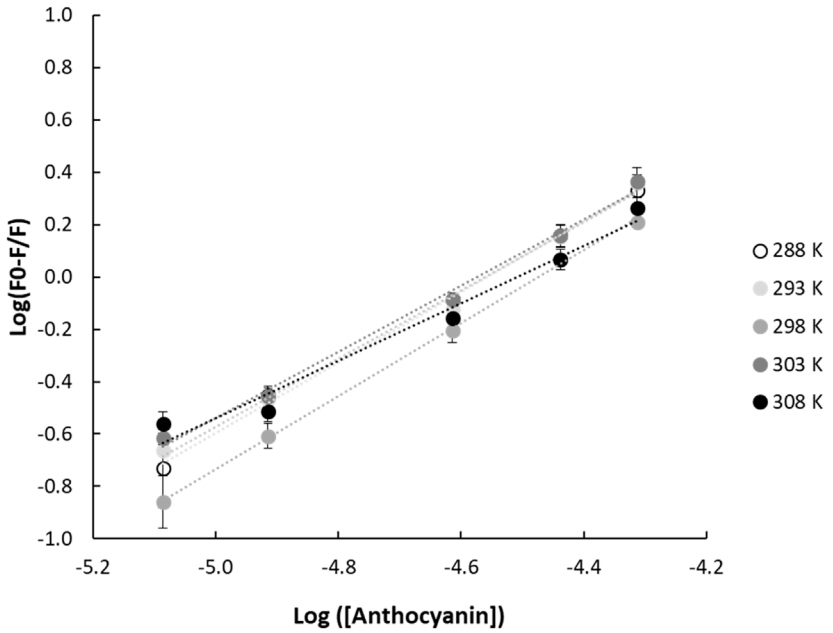

FIGURE 2 | Double logarithmic linear regression plots of (F_0-F/F) and anthocyanin concentration for gliadin-anthocyanin samples measured at different temperatures. F_0 and F are the fluorescence emission intensities of the protein in the absence and presence of quencher, respectively.

Paul et al., 2013). The amplitude average lifetime was calculated as follows (Lakowicz, 1999):

$$\tau_{a0} = \frac{\sum_i \alpha_i \tau_i^2}{\sum_i \alpha_i} \quad (3)$$

The independent lifetimes of all prolamins-ACN combinations did not decrease as ACN concentration increases (**Table 1**, **Supplementary Table S1**). This suggests that the quenching mechanism for the various prolamin-ACN solutions is predominantly static, although dynamic quenching may still occur concurrently but contributes less to the quenching process (Lakowicz, 1999; Paul et al., 2013). It should be noted, however, that the amplitude-weighted lifetime τ_{a0} for all prolamin-ACN combinations decreased significantly as ACN concentration increased. This suggests that resonance energy transfer contributes to the decrease of Trp fluorescence intensity (Paul et al., 2013), that ACNs are in close proximity of the Trp of prolamins, and that ACN-prolamin complexes are formed. The quantitative assessment and the nature of the interactions at the basis of these ACN-prolamin complexes can be further explored through the evaluation of the binding constants and thermodynamic parameters.

DISCUSSION

Non-covalent interactions between proteins and small molecules can take several forms: ionic interaction, hydrogen bonding, van der Waals interaction, as well as the hydrophobic effect (Acharya et al., 2013; Paul et al., 2013; Joye et al., 2015). The ACN-prolamin interactions can be quantitatively assessed in terms of the binding constant (K). Assuming only static quenching occurs, the binding constant

TABLE 2 | Binding and thermodynamic parameters of the quenching of intrinsic prolamin fluorescence by anthocyanins as function of temperature.

Temperature (K)	n	K (M^{-1})	ΔG (J mol^{-1})	ΔH (kJ mol^{-1})	ΔS (J mol^{-1} K^{-1})
Gliadin					
288	1.35 ± 0.081	1.71E+06 ± 1.37E+06	−1.39E+05	−8.66E+01 ± 2.30E+01	1.80E+02 ± 7.49E+01
293	1.25 ± 0.036	9.44E+05 ± 3.38E+05	−1.40E+05		
298	1.38 ± 0.033	1.51E+06 ± 5.33E+05	−1.40E+05		
303	1.26 ± 0.014	6.13E+05 ± 1.14E+05	−1.41E+05		
308	1.10 ± 0.046	9.34E+04 ± 3.66E+04	−1.42E+05		
Hordein					
288	1.35 ± 0.059	1.73E+06 ± 8.47E+05	−4.66E+04	−3.22E+01 ± 1.98E+01	5.02E+01 ± 1.99E+01
293	1.30 ± 0.032	8.32E+05 ± 2.51E+05	−4.69E+04		
298	1.31 ± 0.085	1.15E+06 ± 7.71E+05	−4.71E+04		
303	1.31 ± 0.065	1.01E+05 ± 7.60E+05	−4.74E+04		
308	1.26 ± 0.014	6.14E+05 ± 1.11E+05	−4.76E+04		
Secalin					
288	1.27 ± 0.057	6.66E+05 ± 3.29E+05	−3.14E+04	7.41E+01 ± 1.60E+01	3.67E+02 ± 5.40E+01
293	1.30 ± 0.033	8.31E+05 ± 2.10E+05	−3.32E+04		
298	1.32 ± 0.050	1.26E+06 ± 6.84E+05	−3.51E+04		
303	1.35 ± 0.034	1.75E+06 ± 5.41E+05	−3.69E+04		
308	1.46 ± 0.048	6.07E+06 ± 3.96E+06	−3.87E+04		
Avenin					
288	1.33 ± 0.033	9.10E+05 ± 8.47E+05	−3.25E+04	2.92E+01 ± 2.05E+01	2.14E+02 ± 6.80E+01
293	1.29 ± 0.043	8.22E+05 ± 2.51E+05	−3.35E+04		
298	1.33 ± 0.032	1.22E+06 ± 7.72E+05	−3.46E+04		
303	1.37 ± 0.063	1.79E+06 ± 7.60E+05	−3.57E+04		
308	1.36 ± 0.015	1.63E+06 ± 1.11E+05	−3.67E+04		

(K) associated with the ACN-prolamin interaction can be determined through:

$$\log\left[\frac{F_o - F}{F}\right] = \log K + n\log[Q]$$

in which n is the number of binding sites (Lakowicz, 1999; Paul et al., 2013) (**Figure 2**, **Supplementary Figure S5**). K and n values for all prolamins as a function of temperature are given in **Table 2**. The apparent binding constants for prolamin and ACNs are in line with previously reported binding constants for protein and polyphenols (Acharya et al., 2013; Joye et al., 2015). The binding constants for gliadin-ACN and hordein-ACN interactions decreased as temperature increased, while the corresponding constants for secalin-ACN and avenin-ACN increased. In other words, gliadin-ACN and hordein-ACN interactions become less favorable and the stability of the formed complexes decreased as temperature increased. The interactions are, hence, presumably van der Waals, hydrogen bond or ionic interactions. In contrast, secalin-ACN and avenin-ACN interactions become more favorable and the stability of the formed complexes increased as temperature increased, suggesting that these complexes are stabilized through the hydrophobic effect. Therefore, the functionality of these prolamins on forming colloidal delivery system for ACNs is affected by temperature. In other words, matrix properties and their processing and storage conditions have to be taken into account when incorporating prolamin-based colloidal ACN delivery systems in food products.

The Stern-Volmer plots of gliadin, avenin, hordein and secalin in the presence of increasing concentration of ACN (**Figure 1B**, **Supplementary Figure S3**) show a non-monotonic effect of temperature. A progressive reduction or increase in quenching as temperature increases would indicate static or dynamic quenching, respectively (Lakowicz, 1999). This non-monotonic effect of temperature on the fluorescence quenching suggests that the different prolamins undergo conformational changes in the presence of ACNs as temperature increases (Chang and Lee, 1984).

Assuming that the mechanism of ACN-induced quenching of the intrinsic fluorescence of prolamins is caused predominantly by static quenching, the thermodynamic parameters (ΔG, ΔH, and ΔS) can be calculated to gain insight into the nature of binding between ACNs and the various prolamins. The signs and magnitudes of the thermodynamic parameters for ACN-prolamin interaction provide insight into the nature of the interaction between ACNs and prolamins. Assuming there is no significant variance of change in enthalpy (ΔH) on the temperature range studied, the change in enthalpy and entropy (ΔH and ΔS) can be determined from the Van't Hoff plot equation:

$$\ln[K] = -\frac{\Delta H}{RT} + \frac{\Delta S}{R}$$

where R is the universal gas constant, and T is the temperature in Kelvin (Acharya et al., 2013; Paul et al., 2013). ΔH and ΔS can be estimated from the slope and y-intercept of the plot $ln(K)$ as a function of $1/T$ (Acharya et al., 2013; Paul et al., 2013; Joye et al., 2015) (**Figure 3**). The free Gibbs energy (ΔG) can then be calculated by:

$$\Delta G = \Delta H - T\Delta S$$

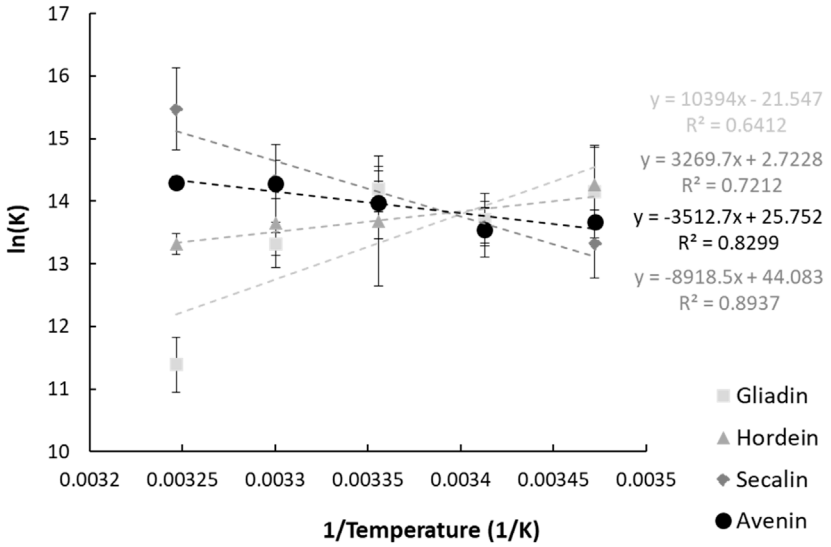

FIGURE 3 | Vant Hoff plots of the interaction between anthocyanins and the four prolamin proteins. The parameters and goodness of fit measures will be better presented in a table.

The obtained thermodynamic parameters for ACN-prolamin interactions are shown in **Table 2**. The Gibbs free energy is negative for all four prolamins, which indicates that the interactions between the four prolamins and ACNs are spontaneous. The negative ΔH for gliadin and hordein indicates that the interactions between gliadin/hordein and ACNs are exothermic, while the interactions between avenin/secalin and ACNs are endothermic (i.e., positive ΔH). The positive entropy (ΔS) for the prolamin proteins shows that the solvent molecules surrounding the prolamin proteins arrange themselves in less orderly fashion when the prolamin interactions with ACNs occur (Joye et al., 2015).

As Ross and Subramanian (1981) described the thermodynamic parameters per non-covalent interaction and based on their findings, we assume that the negative change in enthalpy and positive change in entropy indicate that ionic interactions drive the gliadin-ACN and hordein-ACN interaction. In contrast, the positive enthalpy and entropy change suggest that the predominant interaction processes of secalin-ACN and avenin-ACN are through the hydrophobic effect. The flavylium core of anthocyanins would accommodate interactions driven by the hydrophobic effect. The hydrophobic effect was also found to be the main interaction type for ACN-whey protein systems (Ren and Giusti, 2021) and ACN-black soybean protein isolate systems (Wang and Xie, 2019). Very recently, Guo et al. (2022) studied the interactions between gliadin and grape skin ACN extracts and also reported the hydrophobic effect to be the dominant type of interaction.

The predominant nature of the interaction between the prolamins and ACNs is further substantiated by studying the zeta-potential and hydrophobicity of the prolamins. Gliadin, hordein, and secalin show a positive zeta-potential, with secalin having the smallest magnitude of zeta-potential (**Table 3**). In contrast, under the test conditions, 0.1% w/v avenin, and the bilberry extract have a negative zeta-potential below -9 mV. Therefore, gliadin and hordein (zeta-potential of 11.93 and 8.18 mV) are able to interact with bilberry ACN extract (zeta-potential of -9.46 mV) through attractive electrostatic forces. However, the small magnitude of the zeta-potential of secalin may minimize the electrostatic attraction between secalin and ACNs in BE.

TABLE 3 | Zeta-potential of prolamin [0.10% (w/v)] and bilberry [0.50% (w/v)] extract (BE).

Sample	Zeta-potential (mV)
Gliadin	11.93 ± 0.76a
Hordein	8.18 ± 0.29b
Secalin	2.87 ± 0.11c
Avenin	–9.98 ± 0.20d
Bilberry anthocyanins (BE)	–9.46 ± 2.14d

RP-HPLC chromatograms for gliadin, hordein, secalin, and avenin were divided into sections differing in hydrophobicity and in accordance with the groups identified by Wieser and Belitz (Wieser and Belitz, 1989) (**Figure 4**). Since the prolamin extracts have different protein concentrations, the elution times, rather than the peak intensities, were compared among the different prolamins. The RP-HPLC chromatograms show that the gliadin extract had more polar proteins (classified in the chromatogram as ω-gliadin) than the other prolamin extracts because the first major group of proteins was already eluting ~18 min after injection. In addition, the RP-HPLC chromatograms for gliadin and secalin extracts showed a shoulder ~48 min after injection in the chromatogram. This shows that gliadin and secalin extracts have more apolar proteins than the other prolamin extracts. However, avenin proteins, in general, seem to elute later, indicating the hydrophobic nature of these proteins

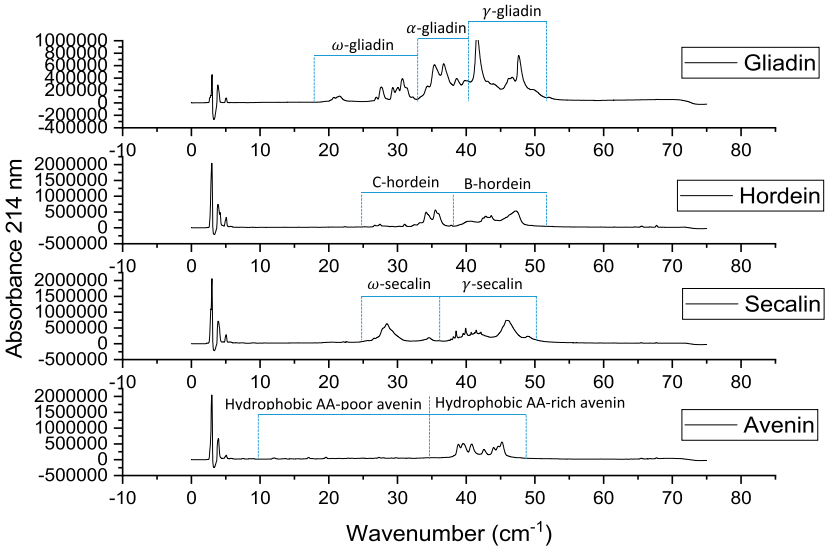

FIGURE 4 | Reverse-phase HPLC chromatograms of gliadin (1.00% w/v), hordein (1.01% w/v), secalin (0.87% w/v), and avenin (0.59% w/v) extracts.

relative to the other prolamins. As such, also the RP-HPLC results for avenin support the fluorescence quenching-derived assumptions on the dominant form of interaction.

This study was able to identify a dominant interaction type between ACNs in BE and each of the prolamins. A molecular docking study would be needed to confirm these findings and gain further insight into the (other) interaction types and molecular arrangement of anthocyanins and prolamins. Furthermore, a commercial extract of bilberries was used here as the anthocyanin source. However, not all components present in this extract are anthocyanins and other components (such as proteins or small sugar molecules) may have contributed to the observed results.

In conclusion, this study relied on fluorescence quenching results to explore the interaction of ACNs with different prolamins. Although prolamins as hydrophobic plant proteins have gained a lot of attention as a matrix material for encapsulation systems for bioactives, to consolidate their potential, more understanding is needed regarding the dominant interaction type driving encapsulation. The four studied prolamins, surprisingly, interact differently with ACNs. While gliadin and hordein interact through ionic interactions, secalin and avenins interaction with ACN seems to be predominantly driven by the hydrophobic effect. The gathered insights illustrate the versatility of these proteins and the need of this understanding as a sound basis for the rational design of encapsulation systems that perform well in terms of encapsulation, controlled release and/or retention of bioactives in a specific food context. The significance of this study lies in 1) the unique combination of minimally invasive steady-state and time-resolved fluorescence analyses to unravel the interactions between ACN and prolamins, and 2) the fundamental insights in the dominant interaction types between ACN, an unstable but economically important natural colorant and bioactive, and prolamins, a group of proteins with unique properties making them highly suitable to conveniently produce encapsulation vehicles for a range of bioactives. These insights will be crucial for future development of powerful protective encapsulation systems for ACN for a range of food applications.

DATA AVAILABILITY STATEMENT

The original contributions presented in the study are included in the article/**Supplementary Material**, further inquiries can be directed to the corresponding authors.

AUTHOR CONTRIBUTIONS

JS: Conceptualization; Formal analysis; Investigation; Methodology; Validation; Visualization; Writing original draft. AC: Resources; Writing Review and Editing. MC: Formal analysis; Methodology; Validation; Supervision; Visualization; Writing—review and editing. IJ: Conceptualization; Formal analysis; Funding acquisition; Resources; Supervision; Visualization; Writing—review and editing.

FUNDING

The authors acknowledge the Ontario Ministry of Research and Innovation Early Researcher Awards Program and the Natural Sciences and Engineering Research Council of Canada Discovery Program for funding this research.

SUPPLEMENTARY MATERIAL

The Supplementary Material for this article can be found online at: https://www.frontiersin.org/articles/10.3389/frfst.2022.889360/full#supplementary-material

REFERENCES

Acharya, D. P., Sanguansri, L., and Augustin, M. A. (2013). Binding of Resveratrol with Sodium Caseinate in Aqueous Solutions. *Food Chem.* 141 (2), 1050–1054. doi:10.1016/j.foodchem.2013.03.037

Arangoa, M. A., Campanero, M. A., Renedo, M. J., Ponchel, G., and Irache, J. M. (2001). Gliadin Nanoparticles as Carriers for the Oral Administration of Lipophilic Drugs. Relationships Between Bioadhesion and Pharmacokinetics. *Pharm. Res.* 18 (11), 1521–1527. doi:10.1023/a:1013018111829

Belitz, H. D., Grosch, W., and Schieberle, P. (2004). *Food Chemistry*. Heidelberg: Springer-Verlag.

Burton-Freeman, B., Sandhu, A., and Edirisinghe, I. (2016). "Anthocyanins," in *Nutraceuticals: Efficacy, Safety and Toxicity*. Editor R. C. Gupta (London, UK: Academic Press), 489–500. doi:10.1016/b978-0-12-802147-7.00035-8

Cassidy, A., Bertoia, M., Chiuve, S., Flint, A., Forman, J., and Rimm, E. B. (2016). Habitual Intake of Anthocyanins and Flavanones and Risk of Cardiovascular Disease in Men. *Am. J. Clin. Nutr.* 104, 587–594. doi:10.3945/ajcn.116.133132.587

Chang, G.-G., and Lee, H.-J. (1984). Monitoring Protein Conformational Changes by Quenching of Intrinsic Fluorescence. *J. Biochem. Biophysical Methods* 9, 351–355. doi:10.1016/0165-022X(84)90019-8

Chung, C., Rojanasasithara, T., Mutilangi, W., and McClements, D. J. (2015). Enhanced Stability of Anthocyanin-Based Color in Model Beverage Systems Through Whey Protein Isolate Complexation. *Food Res. Int.* 76, 761–768. doi:10.1016/j.foodres.2015.07.003

Forester, S. C., and Waterhouse, A. L. (2008). Identification of Cabernet Sauvignon Anthocyanin Gut Microflora Metabolites. *J. Agric. Food Chem.* 56, 9299–9304. doi:10.1021/jf801309n

Ghisaidoobe, A., and Chung, S. (2014). Intrinsic Tryptophan Fluorescence in the Detection and Analysis of Proteins: A Focus on Förster Resonance Energy Transfer Techniques. *Ijms* 15 (12), 22518–22538. doi:10.3390/ijms151222518

Guo, Z., Huang, Y., Huang, J., Li, S., Zhu, Z., Deng, Q., et al. (2022). Formation of Protein-Anthocyanin Complex Induced by Grape Skin Extracts Interacting with Wheat Gliadins: Multi-Spectroscopy and Molecular Docking Analysis. *Food Chem.* 385, 132702. doi:10.1016/j.foodchem.2022.132702

He, Z., Zhu, H., Xu, M., Zeng, M., Qin, F., and Chen, J. (2016). Complexation of Bovine β-Lactoglobulin with Malvidin-3-O-Glucoside and its Effect on the Stability of Grape Skin Anthocyanin Extracts. *Food Chem.* 209, 234–240. doi:10.1016/j.foodchem.2016.04.048

Hubbermann, E. M., Heins, A., Stöckmann, H., and Schwarz, K. (2006). Influence of Acids, Salt, Sugars and Hydrocolloids on the Colour Stability of Anthocyanin Rich Black Currant and Elderberry Concentrates. *Eur. Food Res. Technol.* 223, 83–90. doi:10.1007/s00217-005-0139-2

Joye, I. J., Davidov-Pardo, G., Ludescher, R. D., and McClements, D. J. (2015). Fluorescence Quenching Study of Resveratrol Binding to Zein and Gliadin: Towards a More Rational Approach to Resveratrol Encapsulation Using Water-Insoluble Proteins. *Food Chem.* 185, 261–267. doi:10.1016/j.foodchem.2015.03.128

Keppler, J. K., Stuhldreier, M. C., Temps, F., and Schwarz, K. (2014). Influence of Mathematical Models and Correction Factors on Binding Results of Polyphenols and Retinol with β-Lactoglobulin Measured with Fluorescence Quenching. *Food Biophys.* 9, 158–168. doi:10.1007/s11483-013-9328-x

Kimble, R., Keane, K. M., Lodge, J. K., Howatson, G., Kimble, R., Keane, K. M., et al. (2018). Dietary Intake of Anthocyanins and Risk of Cardiovascular Disease: A Systematic Review and Meta-Analysis of Prospective Cohort Studies. *Crit. Rev. Food Sci. Nutr.* 59 (0), 3032–3043. doi:10.1080/10408398.2018.1509835

Lakowicz, J. R. (1999). "Principles of Fluorescence Spectroscopy," in *Principles of Fluorescence Spectroscopy* (New York, NY: Springer). doi:10.1007/978-1-4757-3061-6

Lakowicz, J. R. (2006). *Principles of Fluorescence Spectroscopy*. New York: Springer Science+Business Media.

Patel, A. R., Heussen, P. C. M., Hazekamp, J., Drost, E., and Velikov, K. P. (2012). Quercetin Loaded Biopolymeric Colloidal Particles Prepared by Simultaneous Precipitation of Quercetin With Hydrophobic Protein in Aqueous Medium. *Food Chem.* 133, 423–429. doi:10.1016/j.foodchem.2012.01.054

Paul, B. K., Ray, D., and Guchhait, N. (2013). Unraveling the Binding Interaction and Kinetics of a Prospective Anti-HIV Drug With a Model Transport Protein: Results and Challenges. *Phys. Chem. Chem. Phys.* 15 (4), 1275–1287. doi:10.1039/c2cp42539d

Prior, R. L., and Wu, X. (2006). Anthocyanins: Structural Characteristics that Result in Unique Metabolic Patterns and Biological Activities. *Free Radic. Res.* 40 (10), 1014–1028. doi:10.1080/10715760600758522

Ren, S., and Giusti, M. M. (2021). Monitoring the Interaction Between Thermally Induced Whey Protein and Anthocyanin by Fluorescence Quenching Spectroscopy. *Foods* 10 (2), 310. doi:10.3390/foods10020310

Ross, P. D., and Subramanian, S. (1981). Thermodynamics of Protein Association Reactions: Forces Contributing to Stability. *Biochemistry* 20 (11), 3096–3102. doi:10.1021/bi00514a017

Skrt, M., Benedik, E., Podlipnik, Č., and Ulrih, N. P. (2012). Interactions of Different Polyphenols With Bovine Serum Albumin Using Fluorescence Quenching and Molecular Docking. *Food Chem.* 135, 2418–2424. doi:10.1016/j.foodchem.2012.06.114

Sui, X., Dong, X., and Zhou, W. (2014). Combined Effect of pH and High Temperature on the Stability and Antioxidant Capacity of Two Anthocyanins in Aqueous Solution. *Food Chem.* 163, 163–170. doi:10.1016/j.foodchem.2014.04.075

Tresserra-Rimbau, A., Rimm, E. B., Medina-Remón, A., Martínez-González, M. A., de la Torre, R., Corella, D., et al. (2014). Inverse Association Between Habitual Polyphenol Intake and Incidence of Cardiovascular Events in the PREDIMED Study. *Nutr. Metabolism Cardiovasc. Dis.* 24, 639–647. doi:10.1016/j.numecd.2013.12.014

Viljanen, K., Kylli, P., Hubbermann, E.-M., Schwarz, K., and Heinonen, M. (2005). Anthocyanin Antioxidant Activity and Partition Behavior in Whey Protein Emulsion. *J. Agric. Food Chem.* 53, 2022–2027. doi:10.1021/jf047975d

Wang, C., and Xie, Y. (2019). Interaction of Protein Isolate with Anthocyanin Extracted from Black Soybean and its Effect on the Anthocyanin Stability. *J. Food Sci.* 84 (11), 3140–3146. doi:10.1111/1750-3841.14816

Wieser, H., and Belitz, H.-D. (1989). Amino Acid Compositions of Avenins Separated by Reversed-Phase High-Performance Liquid Chromatography. *J. Cereal Sci.* 9 (3), 221–229. doi:10.1016/S0733-5210(89)80004-9

Wong, B. T., Zhai, J., Hoffmann, S. V., Aguilar, M.-I., Augustin, M., Wooster, T. J., et al. (2012). Conformational Changes to Deamidated Wheat Gliadins and β-Casein Upon Adsorption to Oil-Water Emulsion Interfaces. *Food Hydrocoll.* 27, 91–101. doi:10.1016/j.foodhyd.2011.08.012

Xiao, J., Nian, S., and Huang, Q. (2015). Assembly of Kafirin/Carboxymethyl Chitosan Nanoparticles to Enhance the Cellular Uptake of Curcumin. *Food Hydrocoll.* 51, 166–175. doi:10.1016/j.foodhyd.2015.05.012

Zhao, C., Giusti, M. M., Malik, M., Moyer, M. P., and Magnuson, B. A. (2004). Effects of Commercial Anthocyanin-Rich Extracts on Colonic Cancer and Nontumorigenic Colonic Cell Growth. *J. Agric. Food Chem.* 52, 6122–6128. doi:10.1021/jf049517a

Conflict of Interest: The authors declare that the research was conducted in the absence of any commercial or financial relationships that could be construed as a potential conflict of interest.